Tracing solar wind plasma entry into the magnetosphere using ion-to-electron temperature ratio

B. Lavraud,[1,2] J. E. Borovsky,[3] V. Génot,[1,2] S. J. Schwartz,[4] J. Birn,[3] A. N. Fazakerley,[5] M. W. Dunlop,[6] M. G. G. T. Taylor,[7] H. Hasegawa,[8] A. P. Rouillard,[6] J. Berchem,[9] Y. Bogdanova,[10] D. Constantinescu,[11] I. Dandouras,[1,2] J. P. Eastwood,[12] C. P. Escoubet,[7] H. Frey,[12] C. Jacquey,[1,2] E. Panov,[13] Z. Y. Pu,[14] C. Shen,[15] J. Shi,[15] D. G. Sibeck,[16] M. Volwerk,[13] and J. A. Wild[17]

Received 5 June 2009; accepted 7 August 2009; published 25 September 2009.

[1] When the solar wind Mach number is low, typically such as in magnetic clouds, the physics of the bow shock leads to a downstream ion-to-electron temperature ratio that can be notably lower than usual. We utilize this property to trace solar wind plasma entry into the magnetosphere by use of Cluster measurements in the vicinity of the dusk magnetopause during the passage of a magnetic cloud at Earth on November 25, 2001. The ion-to-electron temperature ratio was indeed low in the magnetosheath ($T_i/T_e \sim 3$). In total, three magnetopause boundary layer intervals are encountered on that day. They all show that the low ion-to-electron temperature ratio can be preserved as the plasma enters the magnetosphere, and both with and without the observation of Kelvin-Helmholtz activity. This suggests that the ion-to-electron temperature ratio in the magnetopause boundary layer, which is usually high, is not prescribed by the heating characteristics of the plasma entry mechanism that formed these boundary layers. In the future, this property may be used to (1) further trace plasma entry into inner regions and (2) determine the preferred entry mechanisms if other theoretical, observational and simulation works can give indications on which mechanisms may alter this ratio. **Citation:** Lavraud, B., et al. (2009), Tracing solar wind plasma entry into the magnetosphere using ion-to-electron temperature ratio, *Geophys. Res. Lett.*, *36*, L18109, doi:10.1029/2009GL039442.

1. Introduction

[2] The solar wind is decelerated and diverted at the bow shock that forms upstream of the Earth's magnetosphere. The bow shock creates a denser and hotter plasma region that engulfs the magnetosphere: the magnetosheath. It is not the pristine solar wind, but rather the processed magnetosheath plasma, that interacts with the magnetosphere at the magnetopause. Accurate knowledge of the characteristics of the magnetosheath is thus crucial. In particular, its specific properties during low Alfvén Mach number (M_A) drastically alter solar wind – magnetosphere coupling, as described by *Lavraud and Borovsky* [2008].

[3] For typical solar wind conditions, i.e., high M_A (>6), energy conversion at the bow shock leads to high ion-to-electron (T_i/T_e) temperature ratio. From earlier works on the magnetosheath close to the dayside magnetopause, T_i/T_e appears variable and statistically in the range 6–12 [*Paschmann et al.*, 1993; *Phan et al.*, 1994]. At lower M_A, bow shock properties change. In addition to the decreased compression ratio (<4), which affects the downstream magnetosheath densities and magnetic field, lower M_A leads to lower downstream T_i/T_e. Although with significant scatter in the datasets studied, this trend has been well established [e.g., *Bame et al.*, 1979; *Russell et al.*, 1982; *Thomsen et al.*, 1985; *Schwartz et al.*, 1988].

[4] With significant scatter as well, the Earth's central plasma sheet and plasma sheet boundary layers have average $T_i/T_e \sim 7$ [*Baumjohann*, 1993], thus comparable to that in the magnetosheath. The magnetopause boundary layers, inside and directly attached to the magnetopause, contain heated ions and electrons of solar wind origin that have entered the magnetosphere [e.g., *Eastman and Hones*, 1979; *Mitchell et al.*, 1987]. The main processes that have been invoked for their formation are related to magnetic reconnection, diffusive entry and the Kelvin-Helmholtz (KH) instability [e.g., *Dungey*, 1961; *Song and Russell*, 1992; *Lee et al.*, 1994; *Terasawa et al.*, 1997; *Fujimoto et al.*, 1998; *Sibeck et al.*, 1999; *Hasegawa et al.*, 2004; *Nykyri et al.*, 2006; *Lavraud et al.*, 2006]. A question that naturally arises is whether T_i/T_e in the plasma sheet and boundary layers is set (1) by the heating properties of the plasma entry

[1]Centre d'Etude Spatiale des Rayonnements, Université de Toulouse, Toulouse, France.
[2]UMR 5187, Centre National de la Recherche Scientifique, Toulouse, France.
[3]Space Science and Applications, Los Alamos National Laboratory, Los Alamos, New Mexico, USA.
[4]Blackett Laboratory, Imperial College London, London, UK.
[5]Mullard Space Science Laboratory, University College London, Dorking, UK.
[6]Rutherford Appleton Laboratory, Didcot, UK.
[7]ESTEC, ESA, Noordwijk, Netherlands.
[8]Institute of Space and Astronautical Science, JAXA, Sagamihara, Japan.
[9]IGPP, UCLA, Los Angeles, California, USA.
[10]Department of Physics, La Trobe University, Melbourne, Victoria, Australia.
[11]Institut für Geophysik und Extraterrestrische Physik, Technische Universität Braunschweig, Braunschweig, Germany.
[12]Space Sciences Laboratory, University of California, Berkeley, California, USA.
[13]Space Research Institute, Graz, Austria.
[14]School of Earth and Space Sciences, Peking University, Beijing, China.
[15]Center for Space Science and Applied Research, Chinese Academy of Sciences, Beijing, China.
[16]NASA GSFC, Greenbelt, Maryland, USA.
[17]Department of Communication Systems, Lancaster University, Lancaster, UK.

0094-8276/09/2009GL039442$05.00

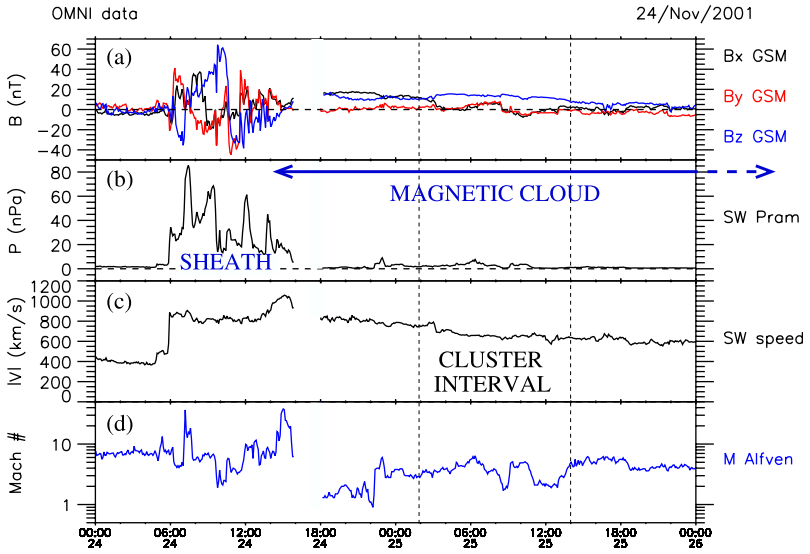

Figure 1. Interplanetary observations during the passage of a magnetic cloud at Earth on November 24–26, 2001 showing the solar wind (a) IMF components in GSM, (b) ram pressure, (c) speed, and (d) Alfvén Mach number.

processes or (2) simply by the temperature ratio of the source magnetosheath, if this ratio is preserved as magnetosheath plasma enters the magnetosphere.

[5] In this paper, we study a Cluster encounter with the dusk side magnetopause during the passage of a low M_A magnetic cloud. It demonstrates that a low ion-to-electron temperature ratio may indeed be preserved upon entry into the boundary layers.

2. Instrumentation

[6] We utilize data from the ion (CIS/HIA [*Rème et al.*, 2001]), electron (PEACE [*Johnstone et al.*, 1997]), and magnetic field (FGM [*Balogh et al.*, 2001]) instruments onboard Cluster spacecraft 1. We use 4 s onboard ion and electron moments. Electron moments were corrected for the spacecraft potential and energy cutoffs as explained by *Génot and Schwartz* [2004]; they are consistent with the lower resolution on-ground moments. We also use OMNI solar wind data (from the ACE spacecraft) to provide the context of Cluster observations. Only GSM coordinates are used.

3. Observations

[7] Figure 1 shows the solar wind context of the Cluster observations. A magnetic cloud passed by Earth between 14 UT on November 24 and 11 UT on November 26, 2001 (blue horizontal arrow). It was preceded by a strong shock and an extended sheath region with large dynamic pressure (Figure 1b). The magnetic field in the sheath was fluctuating and strong, leading to an intense geomagnetic storm ($Dst < -200$ nT; not shown). The magnetic cloud had a very high speed (Figure 1c), explaining the strong compression ahead of it. The leading portion of the core of the magnetic cloud was less geoeffective since it had a less intense and northward magnetic field. The magnetic cloud is characterized by a strong magnetic field but a density significantly lower than the sheath; consequently M_A was low (~2–5; Figure 1d).

[8] Cluster instrumentation was only operational during the interval delimited by the vertical dashed lines in Figure 1, i.e., when M_A was low. For reference, Cluster location was (−3.4, 18.0, −5.2) Earth Radii (GSM) around 09 UT on November 25, i.e., on the dusk-side southern flank just tailward of the dawn-dusk terminator. As will be obvious later from the data, Cluster was always located near the dusk magnetopause, moving from north to south across the equatorial plane near its apogee.

[9] Figures 2a–2f show Cluster data for the interval of operation. The spacecraft first observed wave activity, which we analyse in more detail later. Around 03:30 UT, the spacecraft entered the magnetosheath, characterized by larger tailward flow, higher density and northward magnetic field (Figures 2e, 2b, and 2f). The low density (a few cm^{-3}, a result of the low M_A) and northward magnetic field in the magnetosheath were consistent with the solar wind conditions (Figure 1). The spacecraft entered back into the magnetosphere through the magnetopause on two more occasions, at the times indicated with vertical dashed lines. These re-entries correlate with drops in the solar wind density, observed as short periods of $M_A \sim 2$ in Figure 1d.

[10] The data that constitute the prime focus of the present paper is the ion-to-electron temperature ratio plotted in Figure 2d. It shows that T_i/T_e was unusually low in the magnetosheath. It was generally around 3, as compared to typical values being well above 6 in this region for high M_A [*Paschmann et al.*, 1993; *Phan et al.*, 1994]. A short period of larger density around 6:20 UT, which corresponds to a slightly higher M_A (~5–6 in Figure 1), shows a localised increase of T_i/T_e to about 5. A second high T_i/T_e period is observed in the magnetosheath after ~13:10 UT, which appears related to particle leakage from the magnetopause.

[11] The key observation in Figure 2 is the low T_i/T_e in parts of the boundary layer intervals. Indeed, while fluctuations of T_i/T_e were measured during the wave activity of the first boundary layer encounter, and in part of the second, the ratio is essentially unchanged at ~3 during the entire last boundary layer interval. This observation demonstrates that T_i/T_e in the boundary layers during low

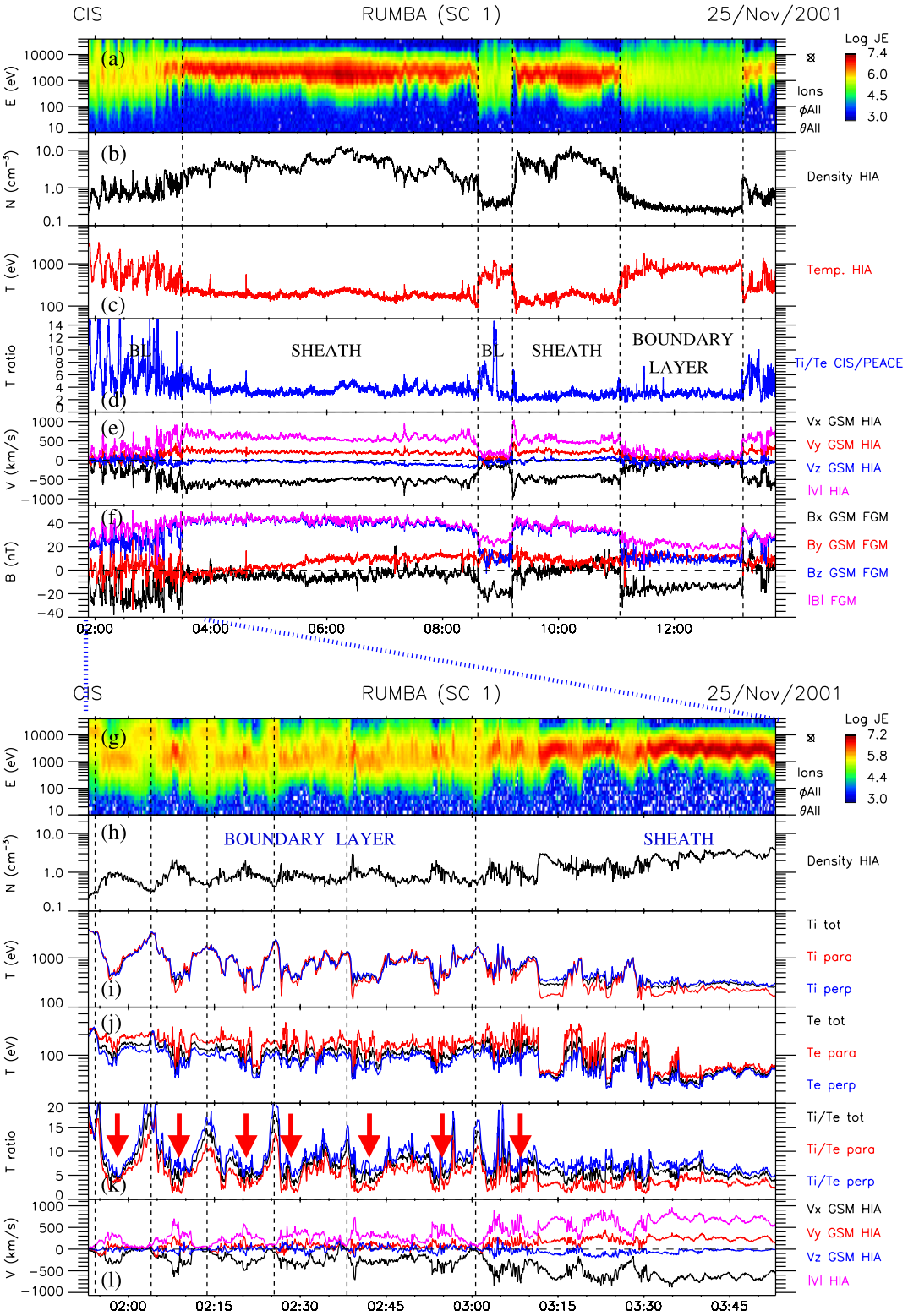

Figure 2. Cluster observations during the period of operation on November 25, 2001. The top panels show (a) the ion omni-directional spectrogram (energy flux), (b) the total ion density, (c) the total ion temperature, (d) the ion-to-electron total temperature ratio, (e) the ion velocity components in GSM, and (f) the magnetic field components in GSM. Three boundary layer intervals were observed, with corresponding magnetopause crossings marked by vertical dashed lines. The bottom panels show (g–l) a zoom of Cluster data during the period of Kelvin-Helmholtz wave activity and (i) the ion and (j) electron temperatures, (k) the ion-to-electron temperature ratios (all for total, parallel and perpendicular components), and (l) the ion velocity component. Times of enhanced T_i/T_e due to the appearance of a hot magnetospheric population are marked by vertical dashed lines. Times of clear boundary layer plasma with low T_i/T_e, similar to that of the magnetosheath are marked with red arrows in Figure 2k.

M_A can be significantly lower than the typical values of either the magnetosheath or plasma sheet during high M_A. As discussed above, this boundary layer (centered at 12 UT) corresponds to an effective $M_A \sim 2$ in the solar wind (Figure 1d). The actual magnetosheath T_i/T_e was not measured at this time. It might have had a somewhat lower T_i/T_e than during the observed magnetosheath intervals where $T_i/T_e \sim 3$, and which corresponded to $M_A \sim 3-4$. These observations yet demonstrate that T_i/T_e inside the magnetosphere can be anomalously low: whatever the plasma entry mechanism, it did not force this ratio to be high.

[12] Wave activity, primarily seen in the magnetic field and flow (Figures 2e and 2f), was often detected in the magnetosheath. Wave activity in the magnetosheath was observed around 8 and 10 UT for instance, together with flow enhancements. No pronounced wave activity was seen inside the last two boundary layer intervals, contrary to the clear activity for the first magnetopause crossing. Figures 2g–2l show a zoom of Cluster data for this crossing. Kelvin-Helmholtz (KH) waves are observed. The waves are characterized by typical anti-correlation between density and temperature (Figures 2h and 2i), and associated flow and magnetic field fluctuations (Figures 2e, 2f, and 2l). Periods with a substantial component of magnetospheric plasma, with low density but large temperatures (Figure 2i), were also observed (vertical dashed lines). Periods of boundary layer plasma, made of heated magnetosheath plasma inside the magnetopause, are highlighted with red arrows. The pristine cold magnetosheath was sampled towards the end of the interval.

[13] Figure 2k shows that while T_i/T_e is high in the pre-existing magnetospheric plasma (vertical dashed lines), in the boundary layer (red arrows) it is of the order of that observed later in the pristine magnetosheath. As explained next, it is unclear whether the KH instability is the process that permitted plasma entry during this event. However, as for the case of the third boundary layer ($\sim$12 UT) T_i/T_e is significantly lower than usual at the times marked by red arrows in this boundary layer. The solar wind M_A is low and steady during this crossing (Figure 1d). Therefore, T_i/T_e was essentially preserved upon entry through the magnetopause.

4. Discussion

[14] The KH waves observed at the first magnetopause crossing on that day were nicely correlated with other spacecraft and ground observations of Pc5 waves in the magnetosphere, as demonstrated by *Rae et al.* [2005]. They identified the Cluster KH observations between 2 and 3 UT as the likely source of the Pc5 waves. For such low M_A conditions, the enhanced tailward flows observed at times in the magnetosheath (e.g., $\sim$3:30–4:00, 7:00–8:30, 9:30–10:00 UT) correspond to enhanced flows adjacent to the magnetopause in the fashion of a slingshot as described in previous works [*Chen et al.*, 1993; *Rosenqvist et al.*, 2007; *Lavraud et al.*, 2007]. As suggested by these authors, such enhanced flows may lead to stronger coupling through enhanced KH activity [cf. also *Lavraud and Borovsky*, 2008].

[15] *Hasegawa et al.* [2006] recently devised a single-spacecraft method to discern KH waves that have entered a non-linear stage and are rolled-up. Using magneto-hydrodynamic simulations they showed that the low density plasma from the magnetospheric side is entrained in rolled-up vortices so as to lead to regions of low density (i.e., of magnetopsheric origin) with tailward velocities larger than the dense magnetosheath itself. They tested and confirmed this property with spacecraft data [cf. also *Taylor et al.*, 2008]. For the present KH wave observations, no clear such signature is found (not shown); it is thus not sure whether plasma entry was locally occurring owing to the KH activity.

[16] Figures 2i–2k show the total, parallel and perpendicular components of the ion and electron temperatures, as well as their ratios. Compatible with previous boundary layer observations for higher M_A [*Hasegawa et al.*, 2003; *Nishino et al.*, 2007a], electrons show parallel temperature anisotropy in the boundary layers while ions are more isotropic. By contrast, ions have a perpendicular anisotropy in the magnetosheath while electrons are more isotropic. This results in temperature ratios that follow similar trends for both components (Figure 2k), with the ratio of the perpendicular temperatures being higher than that for parallel temperatures. As noted by previous authors [e.g., *Lee et al.*, 1994; *Johnson and Cheng*, 1997; *Nishino et al.*, 2007b], these characteristics are possibly the result of wave-particle interactions upon entry through the magnetopause. However, *Taylor and Lavraud* [2008] recently found that boundary layer ions at times may be composed of two superposed cold populations of solar wind origin, each with different temperature anisotropy. The mechanisms that may explain the boundary layer anisotropy characteristics, and that would maintain the low temperature ratios as evidenced here, remain to be fully identified.

[17] Finally, high T_i/T_e (above 10 or so) in Figure 2k marks the sampling of the plasma sheet. This high energy population was observed adjacent to and inside the boundary layers; it was seen as a single population on several occasions (vertical dashed lines). The high T_i/T_e of this population may indicate that it was formed at earlier times under higher M_A conditions; remember that *Baumjohann* [1993] found large scatter in T_i/T_e in the plasma sheet. This high value is also related to the spacecraft being located in the dusk-side magnetosphere. Indeed, high T_i/T_e is expected in the plasma sheet at dusk, and lower ones at dawn, owing to the differential gradient and curvature drifts of ions and electrons in the tail. That a significant high energy ion population exists at dusk more than at dawn has been clearly established in previous works [e.g., *Fujimoto et al.*, 1998; *Nishino et al.*, 2007a]. Mixing of this high energy ion population with the newly entered cold plasma of solar wind origin is often observed, i.e., at times other than the vertical dashed lines and red arrows. The short high T_i/T_e interval in the second boundary layer around 8:45 UT also seems related to mixing. Such times correspond to intermediate values of T_i/T_e, and can be explained by this mixing. This highlights the potential impact of transport processes, in addition to entry mechanisms.

5. Conclusions

[18] We investigated the behavior of the ion-to-electron temperature ratio (T_i/T_e) measured by Cluster in the dusk-side magnetosheath and magnetopause boundary layers for low solar wind Alfvén Mach number (M_A), during the

passage of a magnetic cloud at Earth. The observations showed $T_i/T_e \sim 3$ in the magnetosheath, which is unusually low compared to typical values of order 6–12 for higher M_A. This ratio is similarly low in the magnetopause boundary layers observed during this event. Thus, assuming that the plasma has recently entered these layers through the magnetopause, it has essentially preserved this property. It was not possible to determine with certainty which process formed these boundary layers, i.e., reconnection, diffusion or KH instability. These observations demonstrate, at least for this event, that none of these entry mechanisms forced the temperature ratio to be high. This opens the possibility to distinguish which plasma entry mechanism prevails, e.g., if theoretical, simulation and other observational works can shed light on how each mechanism may influence this ratio. No explicit temperature ratio predictions have been found for these mechanisms in previous works; but it is acknowledged that the literature is prolific on those subjects. In the future, this property may also be used to trace solar wind plasma transport into the inner regions of the magnetosphere, though keeping in mind that the ratio may evolve with transport in the tail owing in particular to the mixing of different populations in response to the differential drifts of ion and electron.

[19] **Acknowledgments.** The authors acknowledge the support of ISSI (Bern, Switzerland) for the organization of a combined Cluster-THEMIS study team. We are grateful for the use the AMDA/CDPP tool which allowed conditional searches of low Mach number intervals. We thank the OMNI data team for providing the solar wind data, as well as the ACE teams.

References

Balogh, A., et al. (2001), The Cluster magnetic field investigation: Overview of in-flight performance and initial results, *Ann. Geophys.*, *19*(10–12), 1207–1217.

Bame, S. J., et al. (1979), High temporal resolution observations of electron heating at the bow shock, *Space Sci. Rev.*, *23*, 75–92, doi:10.1007/BF00174112.

Baumjohann, W. (1993), The near-Earth plasma sheet: An AMPTE/IRM perspective, *Space Sci. Rev.*, *64*, 141–163, doi:10.1007/BF00819660.

Chen, S.-H., M. G. Kivelson, J. T. Gosling, R. J. Walker, and A. J. Lazarus (1993), Anomalous aspects of magnetosheath flow and of the shape and oscillations of the magnetopause during an interval of strongly northward interplanetary magnetic field, *J. Geophys. Res.*, *98*(A4), 5727–5742, doi:10.1029/92JA02263.

Dungey, J. W. (1961), Interplanetary magnetic field and the auroral zones, *Phys. Rev. Lett.*, *6*, 47–48, doi:10.1103/PhysRevLett.6.47.

Eastman, T. E., and E. W. Hones Jr. (1979), Characteristics of the magnetospheric boundary layer and magnetopause layer as observed by IMP 6, *J. Geophys. Res.*, *84*(A5), 2019–2028, doi:10.1029/JA084iA05p02019.

Fujimoto, M., T. Terasawa, T. Mukai, Y. Saito, T. Yamamoto, and S. Kokubun (1998), Plasma entry from the flanks of the near-Earth magnetotail: Geotail observations, *J. Geophys. Res.*, *103*(A3), 4391–4408, doi:10.1029/97JA03340.

Génot, V., and S. J. Schwartz (2004), Spacecraft potential effects on electron moments derived from a perfect plasma detector, *Ann. Geophys.*, *22*(6), 2073–2080.

Hasegawa, H., M. Fujimoto, K. Maezawa, Y. Saito, and T. Mukai (2003), Geotail observations of the dayside outer boundary region: Interplanetary magnetic field control and dawn-dusk asymmetry, *J. Geophys. Res.*, *108*(A4), 1163, doi:10.1029/2002JA009667.

Hasegawa, H., et al. (2004), Rolled-up Kelvin-Helmholtz vortices and associated solar wind entry at Earth's magnetopause, *Nature*, *430*, 755–758, doi:10.1038/nature02799.

Hasegawa, H., M. Fujimoto, K. Takagi, Y. Saito, T. Mukai, and H. Rème (2006), Single-spacecraft detection of rolled-up Kelvin-Helmholtz vortices at the flank magnetopause, *J. Geophys. Res.*, *111*, A09203, doi:10.1029/2006JA011728.

Johnson, J. R., and C. Z. Cheng (1997), Kinetic Alfvén waves and plasma transport at the magnetopause, *Geophys. Res. Lett.*, *24*(11), 1423–1426, doi:10.1029/97GL01333.

Johnstone, A. D., et al. (1997), PEACE: A plasma electron and current experiment, *Space Sci. Rev.*, *79*, 351–398, doi:10.1023/A:1004938001388.

Lavraud, B., and J. E. Borovsky (2008), Altered solar wind-magnetosphere interaction at low Mach numbers: Coronal mass ejections, *J. Geophys. Res.*, *113*, A00B08, doi:10.1029/2008JA013192.

Lavraud, B., M. F. Thomsen, B. Lefebvre, S. J. Schwartz, K. Seki, T. D. Phan, Y. L. Wang, A. Fazakerley, H. Rème, and A. Balogh (2006), Evidence for newly closed magnetosheath field lines at the dayside magnetopause under northward IMF, *J. Geophys. Res.*, *111*, A05211, doi:10.1029/2005JA011266.

Lavraud, B., J. E. Borovsky, A. J. Ridley, E. W. Pogue, M. F. Thomsen, H. Rème, A. N. Fazakerley, and E. A. Lucek (2007), Strong bulk plasma acceleration in Earth's magnetosheath: A magnetic slingshot effect?, *Geophys. Res. Lett.*, *34*, L14102, doi:10.1029/2007GL030024.

Lee, L. C., J. R. Johnson, and Z. W. Ma (1994), Kinetic Alfvén waves as a source of plasma transport at the dayside magnetopause, *J. Geophys. Res.*, *99*(A9), 17,405–17,411, doi:10.1029/94JA01095.

Mitchell, D. G., F. Kutchko, D. J. Williams, T. E. Eastman, L. A. Frank, and C. T. Russell (1987), An extended study of the low-latitude boundary layer on the dawn and dusk flank of the magnetosphere, *J. Geophys. Res.*, *92*(A7), 7394–7404, doi:10.1029/JA092iA07p07394.

Nishino, M. N., M. Fujimoto, T. Terasawa, G. Ueno, K. Maezawa, T. Mukai, and Y. Saito (2007a), Temperature anisotropies of electrons and two component protons in the dusk plasma sheet, *Ann. Geophys.*, *25*(6), 1417–1432.

Nishino, M. N., M. Fujimoto, G. Ueno, T. Mukai, and Y. Saito (2007b), Origin of temperature anisotropies in the cold plasma sheet: Geotail observations around the Kelvin-Helmholtz vortices, *Ann. Geophys.*, *25*(9), 2069–2086.

Nykyri, K., et al. (2006), Cluster observations of reconnection due to the Kelvin-Helmholtz instability at the dawnside magnetospheric flank, *Ann. Geophys.*, *24*(10), 2619–2643.

Paschmann, G., W. Baumjohann, N. Sckopke, T.-D. Phan, and H. Lühr (1993), Structure of the dayside magnetopause for low magnetic shear, *J. Geophys. Res.*, *98*(A8), 13,409–13,422, doi:10.1029/93JA00646.

Phan, T.-D., G. Paschmann, W. Baumjohann, N. Sckopke, and H. Lühr (1994), The magnetosheath region adjacent to the dayside magnetopause: AMPTE/IRM observations, *J. Geophys. Res.*, *99*(A1), 121–141, doi:10.1029/93JA02444.

Rae, I. J., et al. (2005), Evolution and characteristics of global Pc5 ULF waves during a high solar wind speed interval, *J. Geophys. Res.*, *110*, A12211, doi:10.1029/2005JA011007.

Rème, H., et al. (2001), First multispacecraft ion measurements in and near the Earth's magnetosphere with the identical Cluster Ion Spectrometry (CIS) experiment, *Ann. Geophys.*, *19*(10–12), 1303–1354.

Rosenqvist, L., A. Kullen, and S. Buchert (2007), An unusual giant spiral arc in the polar cap region during the northward phase of a coronal mass ejection, *Ann. Geophys.*, *25*, 507–517.

Russell, C. T., M. M. Hoppe, W. A. Livesey, J. T. Gosling, and S. J. Bame (1982), ISEE-1 and -2 observations of laminar bow shocks: Velocity and thickness, *Geophys. Res. Lett.*, *9*(10), 1171–1174, doi:10.1029/GL009i010p01171.

Schwartz, S. J., M. F. Thomsen, S. J. Bame, and J. Stansberry (1988), Electron heating and the potential jump across fast mode shocks, *J. Geophys. Res.*, *93*(A11), 12,923–12,931, doi:10.1029/JA093iA11p12923.

Sibeck, D. G., et al. (1999), Plasma transfer processes at the magnetopause, *Space Sci. Rev.*, *88*, 207, doi:10.1023/A:1005255801425.

Song, P., and C. T. Russell (1992), Model of the formation of the low-latitude boundary layer for strongly northward interplanetary magnetic field, *J. Geophys. Res.*, *97*(A2), 1411–1420, doi:10.1029/91JA02377.

Taylor, M. G. G. T., and B. Lavraud (2008), Observation of three distinct ion populations at the Kelvin-Helmholtz-unstable magnetopause, *Ann. Geophys.*, *26*(6), 1559–1566.

Taylor, M. G. G. T., et al. (2008), The plasma sheet and boundary layers under northward IMF: a multi-point and multi-instrument perspective, *Adv. Space Res.*, *41*(10), 1619–1629, doi:10.1016/j.asr.2007.10.013.

Terasawa, T., et al. (1997), Solar wind control of density and temperature in the near-Earth plasma sheet: Wind/Geotail collaboration, *Geophys. Res. Lett.*, *24*(8), 935–938, doi:10.1029/96GL04018.

Thomsen, M. F., J. T. Gosling, S. J. Bame, and M. M. Mellott (1985), Ion and electron heating at collisionless shocks near the critical Mach number, *J. Geophys. Res.*, *90*(A1), 137–148, doi:10.1029/JA090iA01p00137.

J. Berchem, IGPP, UCLA, 3877 Slichter Hall, 405 Hilgard Avenue, Los Angeles, CA 90095-1567, USA.

J. Birn and J. E. Borovsky, Space Science and Applications, Los Alamos National Laboratory, Los Alamos, NM 87545-0000, USA.

Y. Bogdanova, Department of Physics, La Trobe University, PS1 Building, Melbourne, Vic 3086, Australia.

D. Constantinescu, Institut für Geophysik und Extraterrestrische Physik, Technische Universität Braunschweig, Mendessohnstrasse 3, Braunschweig D-38106, Germany.

I. Dandouras, V. Génot, C. Jacquey, and B. Lavraud, Centre d'Etude Spatiale des Rayonnements, Université de Toulouse, 9 Avenue du Colonel Roche, BP 44346, F-31028 Toulouse CEDEX 4, France. (benoit.lavraud@cesr.fr)

M. W. Dunlop and A. P. Rouillard, Rutherford Appleton Laboratory, Didcot OX11 0QX, UK.

J. P. Eastwood and H. Frey, Space Sciences Laboratory, University of California, 7 Gauss Way, Berkeley, CA 94720-7450, USA.

C. P. Escoubet and M. G. G. T. Taylor, ESTEC, ESA, Noordwijk NL-2200 AG, Netherlands.

A. N. Fazakerley, Mullard Space Science Laboratory, University College London, RH5 6NT Dorking, UK.

H. Hasegawa, Institute of Space and Astronautical Science, JAXA, 3-1-1 Yoshinodai, Sagamihara, 229-8510, Japan.

E. Panov and M. Volwerk, Space Research Institute, Schmiedlstrasse 6, Graz A-8042, Austria.

Z. Y. Pu, School of Earth and Space Sciences, Peking University, 5 Yiheyuan Street, Beijing 100871, China.

S. J. Schwartz, Blackett Laboratory, Imperial College London SW7 2AZ, London, UK.

C. Shen and J. Shi, Center for Space Science and Applied Research, Chinese Academy of Sciences, Beijing 100080, China.

D. G. Sibeck, NASA GSFC, Greenbelt, MD 20771, USA.

J. A. Wild, Department of Communication Systems, Lancaster University, Lancaster LA1 4WA, UK.